Compact chopper spectrometers for pulsed sources

J. Voigt[1], **N. Violini**[1], **W. Schweika**[1,2],

JCNS and PGI, JARA-FIT, Forschungszentrum Jülich GmbH, 52425 Jülich, Germany
European Spallation Source ESS ERIC, Lund, Sweden

Abstract. We report on the opportunities for direct geometry chopper spectrometers (DGCS) by polychromatic illumination of the sample. At pulsed sources the use of multiple initial neutron energies appears naturally, if the repetition rate of chopper in front of the sample is larger than the repetition rate of the source. As a consequence, a large part of the spectrum is measured redundantly with variable energy and momentum transfer resolution. This can be used to optimize a chopper instrument for deep inelastic scattering, relaxing the requirements on the pulse length, by which the sample is illuminated, and on the secondary flight path, while the width of the spectral distribution must be narrowed down. This can open the path to new types of compact direct geometry chopper spectrometers, which need comparably small areas of detector coverage and allow very high repetition rates to provide a high intensity even if sample size and divergence distributions are limited.

1. Introduction

The high peak flux of MW spallation sources allows the preparation of neutron beams with a very well defined spectral width via sophisticated chopper systems. For the short pulse spallation source the very short pulses in particular of thermal and epithermal neutrons even limits the instrument length when balancing energy resolution and intensity. For cold neutrons and at the long pulse spallation source, **P**ulse shaping by the P-chopper can be employed to provide instruments with unprecedented energy resolution. For the long instruments proposed for the ESS, the effective pulse length to realize high energy resolution varies between a few 100 μs for (epi-)thermal neutrons up to the full pulse length of 2.86 ms for cold neutrons.

The mismatch between the period of the neutron source 17 ms $< T_{\mathrm{src}} <$ 100 ms and the typical time needed to record the essential part of the scattered neutron spectrum 1 ms$< T_{\mathrm{frame}} <$ 10 ms can be overcome by using several spectral lines passing through the M-chopper, i.e. the **M**onochromatizing chopper placed as close as possible in front of the sample, which allows the illumination of the sample with a short pulse to resolve the energy of the scattered neutrons by time-of-flight analysis. This has been termed repetition rate multiplication (RRM) [1] or multiple E_i method [2] and happens naturally, when the M chopper spins at a multiple frequency of the source without special precautions.

The instruments at the long pulse spallation sources add now more flexibility to illuminate the samples by discrete polychromatic lines. While 4SEASONS today is using four different lines today, the long pulse of the ESS and a compact secondary spectrometer will allow the use of up to 48 lines. The spacing between subsequent lines $\delta\lambda$ and the instrument bandwidth $\Delta\lambda$ can be chosen, as the instrument length is restricted by the finite pulse length of the source only

for very long wavelength λ and very long instruments:

$$\delta\lambda = \frac{h}{m_n}(f_{\mathrm{M}} L_{\mathrm{M}})^{-1} \quad (1)$$

$$\Delta\lambda = \frac{h}{m_n}(f_{\mathrm{src}} L_{\mathrm{Det}})^{-1}. \quad (2)$$

$L_{\mathrm{Det}} \approx L_{\mathrm{M}}$ denote the distances of the detector and the M chopper, respectively, from the neutron source. In contrast to a monochromatic DGCS, which probes the entire range of energy transfers with the same initial wave vector, one may now illuminate the sample with different wave vectors to cover specific ranges of energy and momentum transfer with ideally matched definitions of the initial and final wave vectors. We will emphasize how this can be used to design a compact spectrometer for high energy transfer, which enables a high illumination rate and an efficient solid angle coverage. The idea has been taken from our developments for the inelastic option of the ESS instrument MAGIC, where it is favorably combined with polarization analysis.

Here we discuss general aspects of compact polychromatic spectrometers, which can achieve very good energy and momentum transfer resolution for deep inelastic scattering.

2. Resolution requirements

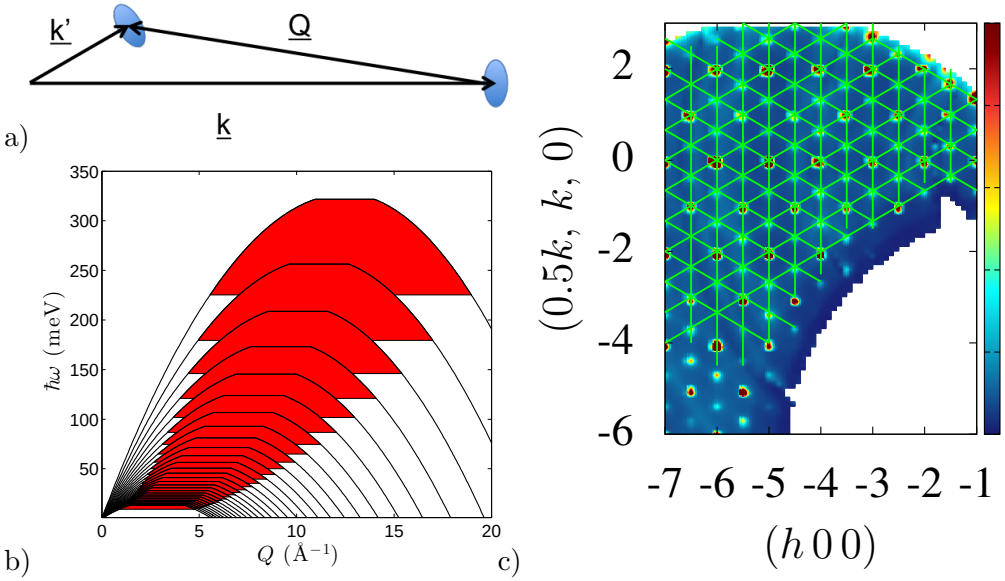

Figure 1. a), b) Kinematics of deep inelastic scattering: (a) Schematic scattering triangle for deep inelastic scattering ($\frac{\hbar\omega}{E_i} = 0.75$). (b) Dynamic range for pulses with 0.5 Å$< \lambda <$ 2.2 Å. The red regions indicate more than 75% energy loss. c) Elastic energy cut through the 4D $S(\vec{Q}, \hbar\omega)$ of the layered Kagome system $CaBaCo_2Fe_2O_7$. The lines indicate Brillouin zone boundaries in the selected plane. The large area, which is probed in reciprocal space, requires a very fine $\vec{Q}$ and hence $\vec{k}$ resolution to probe dispersive features within one Brillouin zone. Courtesy of Johannes Reim [3].

Fig. 1 a) illustrates the scattering triangle and the resolution ellipsoids for the initial and final wave vectors $\vec{k}, \vec{k'}$ for deep inelastic scattering. Note that we use the convention $\hbar\omega > 0$ for neutron energy loss throughout the paper. In particular the initial wave vector must be defined

very precisely in that case. The example in Fig. 1c) shows the huge reciprocal space area that is covered by $k \approx 6\text{Å}^{-1}$. To resolve dispersive features in a Brillouin zone, it is necessary to control the length of the wave vector by the appropriate chopper settings and the direction of the wave vector by a narrow collimation. The new feature of the concept proposed here is clarified in Fig. 1b), which shows the dynamic range covered by the individual discrete pulses: Thanks to the narrowly spaced discrete lines, by which the sample is illuminated, one can explore a large range in energy and momentum transfer by combining the data from the region $\hbar\omega > 0.75E_i$, as indicated by the red areas.

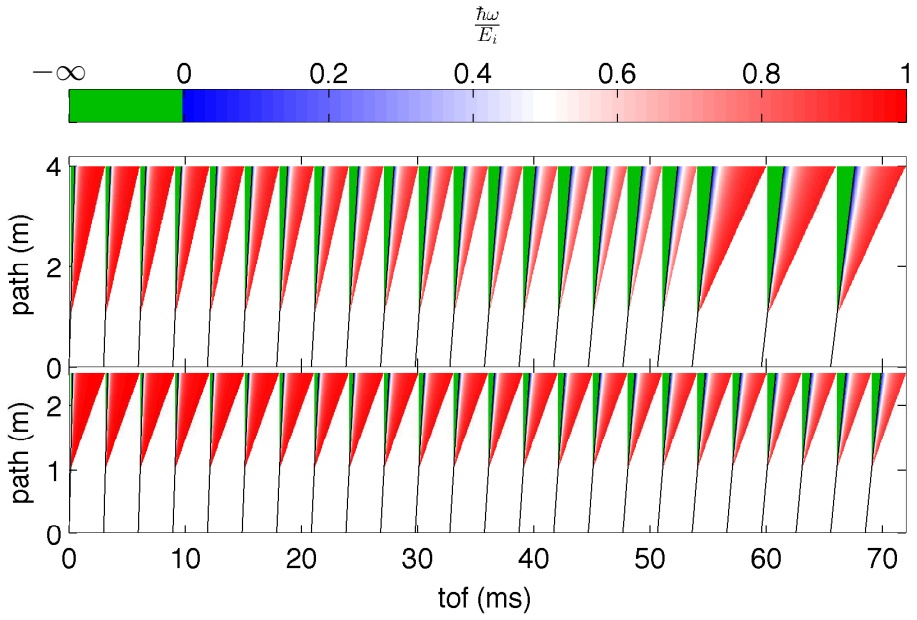

Figure 2. Flight path diagram for a secondary spectrometer with $L_{\text{SD}} = 1.5$ m (bottom) and $L_{\text{SD}} = 3$ m (top) during one ESS pulse. The colors code the relative energy transfer of neutrons arriving at the detector at a certain time.

In Fig. 2 we compare the relative energy transfer, which is recorded at the detector after the illumination through the M-chopper for all sub-pulses within one ESS pulse using a band 0.5 Å$< \lambda <$ 2.2 Åfor different sample-to-detector distances L_{SD}. The reddish colors indicates, that the neutron, which are recorded at the detector have experienced an energy loss of more than 50 %, while blue represents a modest energy loss and green refers to energy gain scattering. Comparing the red and blue fractions for different sample-to-detector distances it is obvious, that the detector closer to the sample records deep inelastic scattering for most of the time. To measure clean spectra up to very high energy transfers, the frame overlap with the up-scattering events from the subsequent pulse must be excluded within the time frame, which is defined by the highest required energy transfer:

$$T_{rec} = \frac{m_n}{h} L_{SD} \lambda \frac{1}{\sqrt{1 - \frac{\hbar\omega_{max}}{E_i}}}, \tag{3}$$

depending on the energy transfer range of interest. In Fig. 2 the criterion $\hbar\omega_{max} = 0.8E_i$ was chosen and therefore three pulses must be suppressed, e.g. by the action of a Fan chopper as suggested by one of the authors in [4].

The energy resolution of a chopper spectrometer can be expressed according to Lechner [5][6] as:

$$\Delta\hbar\omega = \frac{h^3}{m_n^2}\frac{\sqrt{A^2+B^2+C^2}}{\lambda'^3 L_{\mathrm{SD}} L_{\mathrm{PM}}}, \tag{4}$$

with m_n being the mass of neutron, h the Planck's constant,

$$A = \tau_{\mathrm{M}}(L_{\mathrm{PM}} + L_{\mathrm{MS}} + (\lambda'/\lambda)^3 L_{\mathrm{SD}}), \tag{5}$$
$$B = \tau_{\mathrm{P}}(L_{\mathrm{MS}} + (\lambda'/\lambda)^3 L_{\mathrm{SD}}), \tag{6}$$
$$C = \frac{m_n}{h} L_{\mathrm{PM}} \cdot \lambda' \cdot \Delta L, \tag{7}$$

to separate the resolution contributions of the pulse length $\tau_{\mathrm{M}}, \tau_{\mathrm{P}}$ A and B of the initial velocity defining M and P choppers and the flight path uncertainties C, respectively. Here λ, λ' denote the initial and the scattered neutron wavelength and $L_{\mathrm{PM}}, L_{\mathrm{MS}}, L_{\mathrm{SD}}$ the distance between the resolution defining P and M choppers (typically pairs of counter rotating discs), between final M chopper and sample and between sample and detector. A more general treatment of the 4d resolution function of a DGCS can be found in [7], but for the present discussion we assume that the total flight path uncertainties sum up to ΔL.

While shorter $\tau_{\mathrm{M}}, \tau_{\mathrm{P}}$ improve the energy resolution, the intensity passing through the temporal 'slit system' is proportional to the product:

$$F \propto \frac{\tau_{\mathrm{P}} + \tau_{\mathrm{M}}}{L_{\mathrm{PM}}} \times \tau_{\mathrm{M}}. \tag{8}$$

The first term on the right hand side describes the spectral width of the incoming neutron beam and the second term takes into account that the illumination time of the sample must be restricted to analyze the energy transfer by measurement of the secondary time-of-flight. Optimizing the energy resolution under the additional condition of a maximized flux using the method of Lagrange multipliers yields

$$\tau_{\mathrm{P}} = \frac{\tau_{\mathrm{M}}}{2} \times \left(\sqrt{4\left(\frac{L_{\mathrm{PM}} + L_{\mathrm{MS}} + (\lambda'/\lambda)^3 L_{\mathrm{SD}}}{L_{\mathrm{MS}} + (\lambda'/\lambda)^3 L_{\mathrm{SD}}}\right)^2 + 1} - 1 \right). \tag{9}$$

This result is different from Lechner [5], as the flux in eq. (8) depends quadratically on τ_{M}, but linearly on τ_{P}. In the case of $L_{\mathrm{PM}} \gg L_{\mathrm{MS}} + (\lambda'/\lambda)^3 L_{\mathrm{SD}}$ eq. (9) simplifies to

$$\tau_{\mathrm{P}} = \tau_{\mathrm{M}} \times \left(\frac{L_{\mathrm{PM}} + L_{\mathrm{MS}} + (\lambda'/\lambda)^3 L_{\mathrm{SD}}}{L_{\mathrm{MS}} + (\lambda'/\lambda)^3 L_{\mathrm{SD}}} \right) \tag{10}$$

as in [5]. According to eq. (9) the ideal pulse shaping time varies strongly depending on the energy transfer, as shown in Fig. 4, which compares the ideal ratio of τ_{P} and τ_{M} as a function of relative energy transfer for two different sample-to-detector distances and with chopper positions as suggested for the long ESS chopper spectrometers CSPEC and T-REX. With increasing relative energy transfer a shorter pulse length τ_{P} is needed to define the initial wave vector and hence energy more precise. This is evident from Fig. 2, too: For the M-chopper pulses that arrive later within one ESS pulse the fraction of deep inelastic scattering is reduced and therefore the initial wavelength definition can be relaxed, i.e. the pulse length τ_{P} can be increased for later pulses with longer wavelength.

This is exactly the property of a optical blind chopper configuration proposed originally for reflectometers by [8]. Here a pair of disc choppers rotate in the same sense at a certain distance

Z. The phase is set such, that the second chopper only starts opening the beam, when the first chopper finishes closing the beam. As a result, the chopper is closed for infinitely fast neutrons, but for neutrons of finite velocity the choppers can be passed with a pulse length, that increases linearly according to the distance between the choppers:

$$\tau(\lambda) = \tau_{max} - |\tau_{max} - \frac{m_n}{h}\lambda Z| \tag{11}$$

$$\tau_{max} = \frac{w}{2\pi R f} \tag{12}$$

with w denoting the width of the neutron beam, R the radius and f the chopper pair frequency. If the right hand expression of eq. (11) would evaluate negativ, the chopper does not transmit. Recently this concept has been extended by realizing the first and second chopper by pairs of counter rotating choppers to double the speed, by which the beam cross section can be opened and closed [9]. This design not only provides a wavelength dependent pulse length, but decouples the pulse length to a certain extend from the chopper frequency: As the first pair opens the beam and the second pair closes the beam, the pulse length can be adjusted shifting the relative phase ϕ of the two pairs yielding

$$\tau(\lambda) = \tau_{max} - |\tau_{max} - \frac{m_n}{h}(\lambda - \lambda_1)Z| \tag{13}$$

with $\lambda_1 = \frac{h}{m_n}\frac{\phi}{2\pi f Z}$. As seen in Fig. 3 the pulse length passing through a quartet of choppers for a given wavelength varies with the phase between the first pair and the second pair without changing the chopper frequency.

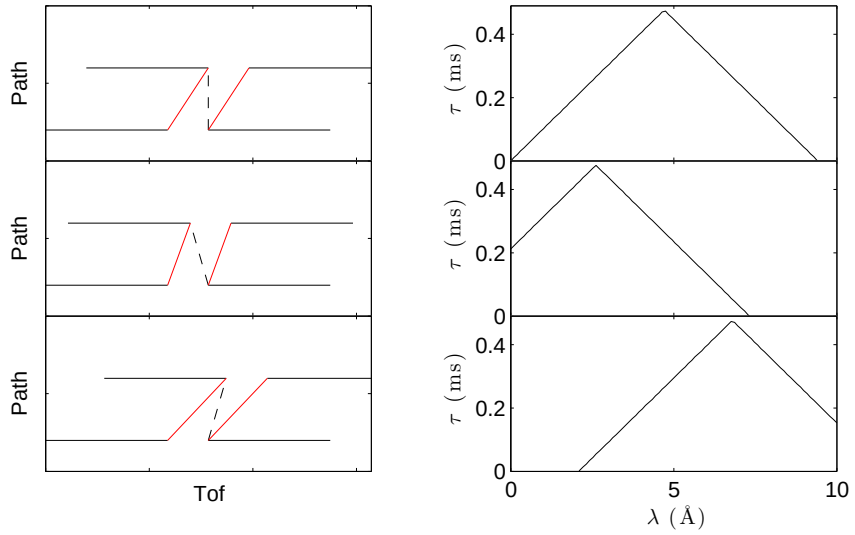

Figure 3. Schematic flight path diagrams (left) for chopper pairs at the distance $Z = 0.4$ m for three different phases and the resulting $\tau(\lambda)$ graphs (right). (top) $\lambda_1 = 0$Å, (center) $\lambda_1 = -2.1$Å, (bottom) $\lambda_1 = 2.1$Å,

For the optimization of the M-chopper pulse length we consider the secondary time-of-flight of the slowest final neutrons, which can be detected without frame overlap:

$$\lambda'_{max} = \frac{h}{m_n}\frac{1 + \frac{L_{\mathrm{MS}}}{L_{\mathrm{PM}}}}{L_{\mathrm{SD}} f_{\mathrm{M}}}. \tag{14}$$

This does not change, if the time frame is not changed, i.e. no pulses are skipped. Hence we keep τ_{M} constant for all pulses.

We evaluate now the resulting energy resolution for a constant $\tau_{\mathrm{M}} = 30\mu$s and varying τ_{P} according to the ratio $\frac{\tau_{\mathrm{P}}}{\tau_{\mathrm{M}}}$ shown in Fig. 4a) in the range from 0.8 $\frac{\hbar\omega}{E_i}$ to 0.5 for the different sample-to-detector distances $L_{\mathrm{SD}} = 1.5, 3$ m. This yields τ_{P} varying from 0.105 ms to 0.285 ms and from 0.06 to 0.166 ms within a band $\Delta\lambda = 1.77$ Å for the assumed instrument length. The pulse length gradient is realized by a distance of 0.4 m and 0.24 m between both P chopper pairs. The slits on each of the four chopper discs must be chosen significantly wider than the beam cross section to enable the variation of the pulse length. This requirement seems technically achievable: First, the pulse length is rather long ($\tau_{\mathrm{P}} > 100\mu$s) and second, the requirement of a narrow divergent beam to achieve a good $\vec{Q}$-resolution will limit the guide dimensions also for a ballistic guide concept (note that the guide cross section of the T-REX spectrometer at the position of the P-chopper, which is 60 mm × 90 mm, can be closed sufficiently fast).

The relaxed resolution for the shorter secondary flight path is fully compensated by a flux gain, as the flux is proportional to τ_{P}. It should be noted, that even the short instrument realizes a resolution of 11 meV for 320 meV excitation energy and 0.4 meV for 18 meV excitation energy. For this sample-to-detector distance a large solid angle coverage is possible with detector areas well below 10 m^2. Concerning line shape investigations the narrowing of the resolution curves matches with usually longer lifetimes of lower energy excitations in contrast to monochromatic DGCS, where the resolution gets broader for lower energy transfer.

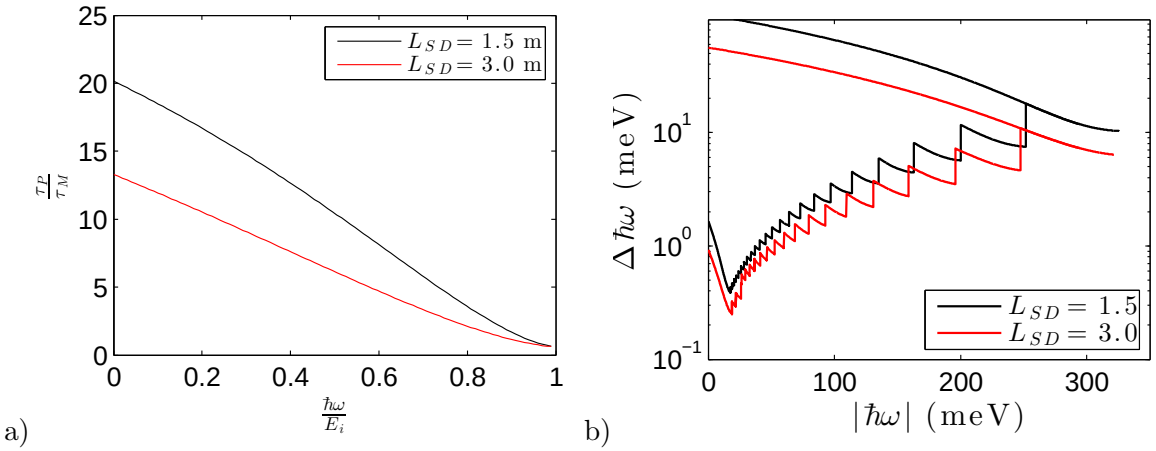

Figure 4. left: Ratio $\frac{\tau_{\mathrm{P}}}{\tau_{\mathrm{M}}}$ as a function of rel. energy transfer. right: Energy resolution as a function of energy transfer for the following parameters: $f_M = 350$ Hz, $L_{\mathrm{M}} = 165$ m, $L_{\mathrm{P}} = 110$ m, $L_{\mathrm{MS}} = 1$ m, $\Delta L = 10$ mm. Except for the highest and lowest energy pulses, only the best resolution for a given energy transfer is displayed.

3. Conclusion

We propose here a new concept for a compact chopper spectrometer optimized for deep inelastic scattering and good momentum transfer resolution. It makes use of the polychromatic illumination of a sample at a pulsed neutron source, where each pulse is optimized to a narrow energy transfer region. The illumination by multiple narrow spectral lines, which is natural at pulsed sources is crucial to explore a large overal dynamical range. The definition of the initial neutron wave vector can be tuned to achieve excellent energy transfer and momentum transfer resolution even by relaxing the timing conditions on the chopper directly in front of the sample, which usually sets the technical limit for the energy resolution. Furthermore the secondary flight path can be reduced to allow an efficient solid angle coverage at reasonable cost.

References

[1] Russina M and Mezei F. 2009 *Nucl. Instr. Meth. A* **604(3)**:624–631.

[2] Nakamura M, Kajimoto R, Inamura Y, Mizuno F, Fujita M, Yokoo T, and Arai M 2009 *Jour. Phys. Soc. Jap.*, **78(9)** 093002.

[3] Reim J 2015 Ph. D. thesis, RWTH Aachen.

[4] Voigt J, Violini N, and Brueckel T 2014. *Nucl. Instr. Meth. A*, **741** 26–32.

[5] Lechner R E 1991 In M. Misawa, M. Furusaka, H. Ikeda, and N. Watanabe, editors, *Proceedings ICANS-IX* KEK.

[6] Lechner R E 1984 In R. Scherm and H. Stiller, editors, *Proceedings "Workshop on neutron scattering instrumentation for SNQ"*, volume Jül-1954. Forschungszentrum Jülich, 1984.

[7] Violini N, Voigt J, Pasini S, and Brueckel T 2014 *Nucl. Instr. Meth. A*, **736** 31–39.

[8] van Well A A 1992 *Physica B: Condensed Matter* **180–181**, Part 2(0):959–961.

[9] Vickery A and Deen P P 2014 *Rev. Sci. Instr.*, **85(11)** 115103.